Rearrangement Pathways of Arylperoxy Radicals. 2. Five-Membered Heterocycles

Michael J. Fadden and Christopher M. Hadad*

Contribution from the Department of Chemistry, The Ohio State University, 100 West 18th Avenue, Columbus, Ohio 43210

Received: March 30, 2000; In Final Form: May 10, 2000

The potential energy surfaces for the reaction of furanyl and oxazolyl radicals with O_2 have been examined using the B3LYP method. The initial production of the arylperoxy radical followed by either simple decomposition or rearrangement to yield several intermediates (aryloxy, dioxiranylaryl, or dioxetanylaryl radicals) has been explored. Transition state structures for most of the steps are presented as well as relative free energies over a range of temperatures from 298 to 2000 K. The energetics of the analogous intermediates for the reaction of O_2 and other five-membered heterocyclic radicals derived from pyrrole and thiophene are also provided. The loss of an O atom is generally the most accessible and energetically favored pathway of decomposition at all temperatures. Dioxiranyl formation is favored over O_2 loss at temperatures $\leq$500 K and favored in the same temperature range over O atom loss in several cases. Dioxetanyl formation incurs the greatest barrier to formation, and direct routes are not available in every molecule surveyed. However, in some cases the dioxetane radicals transform rapidly into very stable species.

I. Introduction

Understanding coal combustion is a challenge because of coal's complex structure and the many functional groups and aromatic rings present in the various ranks of coal.[1] Many researchers have focused on understanding the behavior of model aromatic rings, such as benzene, pyridine, pyrrole, furan, and thiophene, to clarify this complex puzzle. With these model compounds, experimentalists have utilized pyrolysis and oxidative pyrolysis assays in order to provide an understanding of coal combustion.

Many experimental and computational studies have been conducted on the thermal, oxidative pyrolysis of benzene,[2−6] but few studies have been conducted on other aromatic compounds.[7] Of these limited studies, six-membered monocyclic and bicyclic nitrogen-containing aromatic rings have received some attention. Numerous experimental studies have been reported on the pyrolysis of five-membered aromatic heterocycles,[8−12] but none have dealt with oxidative, thermal decomposition. Computational studies[13] have focused on the decomposition of five-membered rings either prior to or after H atom abstraction, but none have dealt with reaction of O_2 prior to decomposition.

Recently, we explored the decomposition of phenyl radical with O_2[14] as well as similar reaction pathways for the analogous decomposition of a wide range of azabenzenes, as depicted in Figure 1.[15] Earlier, we presented a thermodynamic study of the decomposition of arylperoxy radicals derived from furan, pyrrole, and thiophene to yield CO, CO_2, and other smaller hydrocarbons.[16] However, at that time, we were not able to present a complete potential energy surface for decomposition.

In our continued examination of the reactivity of functional groups present in coal, we now turn our attention to a detailed evaluation of five-membered heterocyclic rings (Figure 2). In this study, we examine the potential energy surfaces, including transition states, for the reaction of furan and oxazole with O_2 after H atom abstraction. The thermodynamic free energies from these reaction mechanisms will then be compared to those for thiophene and pyrrole.

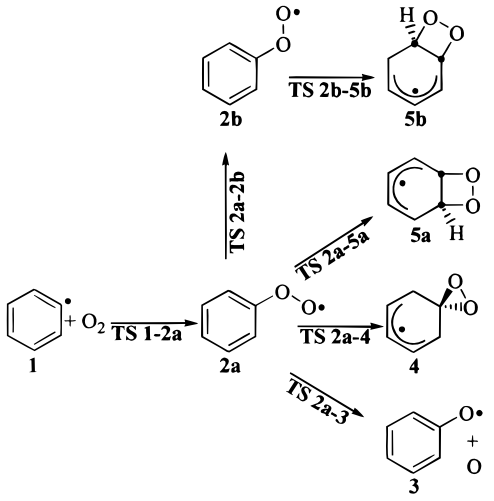

Figure 1. Reaction mechanism for phenyl radical with O_2. This numbering sequence will be used throughout the text, tables, and figures to identify the analogous intermediate and transition state for each five-membered heterocycle.

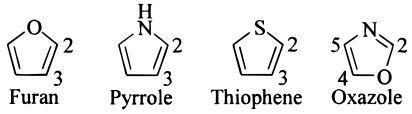

Figure 2. Molecular structures and numbering of furan, pyrrole, thiophene, and oxazole.

II. Computational Methods

All geometry optimizations, vibrational frequency calculations, and single point energy determinations were completed with Gaussian 94 and 98 at the Ohio Supercomputer Center or on our IBM RS/6000 workstations.[17,18]

* Corresponding author. E-mail: hadad.1@osu.edu. Fax: 614-292-1685.

10.1021/jp0012202 CCC: $19.00
Published on Web 06/14/2000

The B3LYP/6-31G* hybrid density functional theory (DFT)[19] level was employed to determine the optimized geometries and vibrational frequencies of all stationary points.[20−23] We,[24] and others,[25] have shown DFT methods can be used to provide accurate energies for aromatic radicals. Single point energies were also determined at the B3LYP/6-311+G** level, as Bauschlicher and Langhoff have shown that there is a small basis set effect with oxygen-containing systems when determining C−H bond dissociation enthalpies,[26] so single point energies were also determined at the B3LYP/6-311+G** level in order to provide better relative energies. We have also determined single point energies at the UCCSD(T)/6-31G** level of theory for several key intermediates and transition states in order to compare with our B3LYP results.[27] All basis sets used six Cartesian *d* functions.

Vibrational frequencies were calculated for each stationary point in order to confirm each structure as a minimum or a saddle point, and each stationary point had the correct number of real and imaginary vibrational frequencies. The zero-point vibrational energy (ZPE) corrections were also obtained and scaled by a factor of 0.9806.[28] All transition states were confirmed to connect to the corresponding reactant and product by displacing (typically 10%) the geometry along the reaction coordinate for the imaginary vibrational frequency in either direction, which was then followed by a careful optimization (opt = calcfc or opt = calcall) to the corresponding minimum. In some cases, intrinsic reaction coordinate (IRC) searches were used.[29]

Spin contamination for most of the stationary points is negligible. The $\langle S^2 \rangle$ values for all of the minima and for most of the transition states fell below 0.80 for these doublet species. Those specific transition states that suffered from excessive spin contamination will be discussed below, and their energies and geometries are considered to be suspect.

To determine the thermodynamic contribution to the free energy of each molecule at temperatures ranging from 298 to 2000 K, Thermo94[30] was used to calculate the partition function contributions derived from the optimized geometry and the unscaled vibrational frequencies as calculated by Gaussian. The overall Gibbs free energy at each temperature was derived from the single point energy, the scaled ZPE, the thermodynamic contribution (enthalpy and entropy), and the electronic contribution to the free energy. The only molecule that received different treatment was the O atom, where experimentally[31] determined splitting energies were included in the electronic component of the partition function for the free energy calculation.

The energies discussed throughout are Gibbs free energies computed at the B3LYP/6-311+G**//B3LYP/6-31G* level (at 298 K, unless noted otherwise), and are relative to the Gibbs free energy of the corresponding arylperoxy radical.

III. Results and Discussion

A. General Reaction Pathways. The reaction pathways explored are shown schematically in Figure 1. The numbering system depicted in Figure 1 will be used in all of the other figures and throughout the text. (For comparative purposes, we have chosen to use the same numbering system as in our recent paper on the oxidative decomposition of the azabenzenes.[15]) The first pathway calculated is O_2 addition to the aryl radical (**1**) in order to form the arylperoxy radical (**2**). The arylperoxy radical may exist as two distinct isomers (**2a** and **2b**), and for our discussion below, the **2a** isomer always represents the more stable isomer. The **2b** isomer will not be shown in cases where the **2b** isomer does not lead to another intermediate or when **2a** = **2b** due to symmetry (as for the phenyl radical).

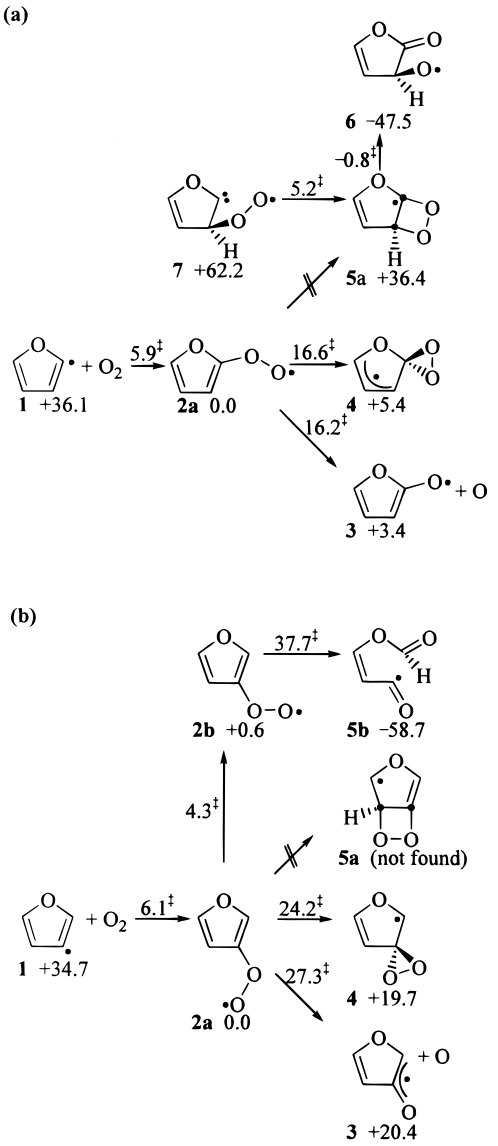

Figure 3. Mechanisms of the (a) 2-furanyl + O_2 and (b) 3-furanyl + O_2 reactions showing Gibbs free energies of activation barriers (relative to the appropriate reactant) and Gibbs free energies of each intermediate at 298 K (relative to the corresponding **2a**) at the B3LYP/6-311+G**//B3LYP/6-31G* level.

We further explored the fragmentation or unimolecular rearrangement of the arylperoxy radical. Loss of an O atom from the arylperoxy radical yields the aryloxy radical (**3**) via O−O bond cleavage. Unimolecular rearrangement pathways can lead to the dioxiranyl radical (**4**) or the dioxetanyl radicals (**5a** and **5b**) via 1,1- and 1,2-addition, respectively. We have previously demonstrated that other pathways (such as 1,3- and 1,4-addition) for the decomposition of the phenylperoxy radical are highly disfavored due to very large activation barriers.[14]

B. Mechanism of the Furanyl Radical + O_2 Reaction. The formation of furanylperoxy radical via the addition of O_2 to furanyl radical initiates the process, as shown in Figure 3. Relative energies are provided in Tables 1 and 2. At 298 K, this reaction is exoergic for both 2- and 3-furanyl radicals by −36.1 and −34.7 kcal/mol, respectively. The free energy of activation ($\Delta G^{\ddagger}$, 298 K) for the formation of either the 2- or 3-furanylperoxy radical is ∼6 kcal/mol. The transition states found for O_2 addition to 2- and 3-furanyl radicals suffer from excessive spin contamination ($\langle S^2 \rangle \sim 1.8$) and have small imaginary vibrational frequencies (19.3*i* and 41.6*i* cm^{-1},

TABLE 1: Gibbs Free Energies (kcal/mol, 298−2000 K) for All Intermediates at the B3LYP/6-311+G//B3LYP/6-31G* Level**

298 K	1	2a	2b	3	4	5a	5b
phenyl	32.3	0.0	*a*	27.3	22.6	44.8	*a*
2-furanyl	36.1	0.0	*b*	3.4	5.4	36.4	*b*
3-furanyl	34.7	0.0	0.6	20.4	19.7	*c*	−58.7
2-oxazolyl	32.3	0.0	0.5	6.3	6.8	*b*	−51.1
4-oxazolyl	34.4	0.0	*b*	3.8	5.8	31.6	*b*
5-oxazolyl	33.6	0.0	1.2	17.9	17.5	−62.0	−20.8
pyrrol-1-yl	−21.1	0.0	*a*	20.8	12.5	28.1	*a*
pyrrol-2-yl	39.9	0.0	3.0	10.2	12.2	*c*	−41.4
pyrrol-3-yl	36.6	0.0	0.2	20.8	21.2	−43.8	−49.5
thiophen-2-yl	33.3	0.0	1.4	9.1	10.5	37.6	*c*
thiophen-3-yl	32.1	0.0	0.1	21.8	20.0	53.6	−46.5
500 K	**1**	**2a**	**2b**	**3**	**4**	**5a**	**5b**
phenyl	24.9	0.0	*a*	20.6	22.8	45.2	*a*
2-furanyl	28.1	0.0	*b*	−3.3	5.7	36.8	*b*
3-furanyl	26.9	0.0	0.6	13.8	19.8	*c*	−59.0
2-oxazolyl	24.5	0.0	0.4	−0.3	7.2	*b*	−50.8
4-oxazolyl	26.6	0.0	*b*	−2.8	6.1	32.2	*b*
5-oxazolyl	25.7	0.0	0.8	11.3	17.6	−62.3	−20.7
pyrrol-1-yl	−28.7	0.0	*a*	14.6	12.7	28.9	*a*
pyrrol-2-yl	31.5	0.0	2.7	3.4	11.7	*b*	−41.8
pyrrol-3-yl	28.7	0.0	0.2	14.3	21.1	−45.7	−49.7
thiophen-2-yl	25.3	0.0	1.3	2.3	10.6	*b*	37.9
thiophen-3-yl	24.2	0.0	0.1	15.2	20.1	53.8	−47.0
1000 K	**1**	**2a**	**2b**	**3**	**4**	**5a**	**5b**
phenyl	7.1	0.0	*a*	3.9	22.9	46.0	*a*
2-furanyl	9.5	0.0	*b*	−19.8	6.0	37.8	*b*
3-furanyl	8.5	0.0	0.7	−2.8	19.6	*c*	−59.7
2-oxazolyl	6.1	0.0	0.3	−16.7	8.1	*b*	−50.0
4-oxazolyl	8.3	0.0	*b*	−19.2	6.6	33.7	*b*
5-oxazolyl	7.3	0.0	0.0	−5.4	17.4	−63.2	−20.7
pyrrol-1-yl	−46.5	0.0	*a*	−0.6	12.9	30.9	*a*
pyrrol-2-yl	11.9	0.0	2.1	−13.4	10.1	*b*	−43.0
pyrrol-3-yl	10.2	0.0	0.3	−2.1	20.6	−50.7	−50.3
thiophen-2-yl	6.5	0.0	1.0	−14.7	10.6	*b*	38.7
thiophen-3-yl	5.7	0.0	0.2	−1.4	20.2	54.2	−48.3
1500 K	**1**	**2a**	**2b**	**3**	**4**	**5a**	**5b**
phenyl	−10.1	0.0	*a*	−12.7	22.8	46.6	*a*
2-furanyl	−8.5	0.0	*b*	−36.3	6.2	38.8	*b*
3-furanyl	−9.2	0.0	0.7	−19.3	19.4	*c*	−60.5
2-oxazolyl	−11.6	0.0	0.1	−33.1	8.9	*b*	−49.2
4-oxazolyl	−9.4	0.0	*b*	−35.6	7.0	35.1	*b*
5-oxazolyl	−10.5	0.0	−0.9	−22.0	17.1	−64.1	−20.8
pyrrol-1-yl	−63.6	0.0	*a*	−15.8	13.0	32.8	*a*
pyrrol-2-yl	−7.0	0.0	1.5	−30.2	8.4	*b*	−44.3
pyrrol-3-yl	−7.6	0.0	0.4	−18.4	19.9	−55.6	−50.9
thiophen-2-yl	−11.7	0.0	0.7	−31.6	10.4	*b*	39.5
thiophen-3-yl	−12.2	0.0	0.3	−17.9	20.1	54.5	−49.6
2000 K	**1**	**2a**	**2b**	**3**	**4**	**5a**	**5b**
phenyl	−26.9	0.0	*a*	−29.3	22.7	47.2	*a*
2-furanyl	−26.1	0.0	*b*	−52.7	6.4	39.8	*b*
3-furanyl	−26.5	0.0	0.8	−35.6	19.0	*c*	−61.4
2-oxazolyl	−28.9	0.0	0.0	−49.4	9.6	*b*	−48.4
4-oxazolyl	−26.7	0.0	*b*	−51.9	7.3	36.5	*b*
5-oxazolyl	−27.8	0.0	−1.8	−38.6	16.7	−65.1	−20.9
pyrrol-1-yl	−80.3	0.0	*a*	−30.7	13.2	34.7	*a*
pyrrol-2-yl	−25.5	0.0	0.9	−46.9	6.6	*b*	−45.6
pyrrol-3-yl	−25.0	0.0	0.5	−34.6	19.1	−60.7	−51.5
thiophen-2-yl	−29.4	0.0	0.4	−48.4	10.2	*b*	40.2
thiophen-3-yl	−29.5	0.0	0.3	−34.3	19.9	54.8	−51.0

[a] Because of symmetry, **2a** = **2b** and **5a** = **5b**. [b] The **2b** isomers were higher in energy and did not lead to any stable isomers. The **5a** or **5b** isomers are not stable, or an analogous product is simply not possible. [c] Despite numerous attempts, this stationary point could not be located at the B3LYP/6-31G* level.

TABLE 2: Free Energies of Activation Leading from Arylperoxy Radicals as a Function of Temperature at the B3LYP/6-311+G//B3LYP/6-31G* Level**

298 K	TS 1-2a	TS 2a-2b	TS 2a-3	TS 2a-4	TS 2a-5a	TS 2b-5b
phenyl	38.4	*a*	51.0	27.2	46.2	*a*
2-furanyl	42.0	*b*	16.2	16.6	*c*	*b*
3-furanyl	40.8	4.3	27.3	24.2	*d*	37.7
2-oxazolyl	37.7	3.3	19.6	20.9	*b*	*c*
4-oxazolyl	50.3	*b*	16.4	17.1	*c*	*b*
5-oxazolyl	49.3	3.8	25.1	24.1	37.6	*b*
500 K	**TS 1-2a**	**TS 2a-2b**	**TS 2a-3**	**TS 2a-4**	**TS 2a-5a**	**TS 2b-5b**
phenyl	34.9	*a*	49.8	27.6	46.9	*a*
2-furanyl	38.1	*b*	16.0	16.9	*c*	*b*
3-furanyl	37.1	5.0	26.1	24.6	*d*	38.4
2-oxazolyl	33.5	4.1	19.5	21.3	*b*	*c*
4-oxazolyl	46.3	*b*	16.3	17.5	*c*	*b*
5-oxazolyl	45.0	4.5	24.5	24.5	38.2	*b*
1000 K	**TS 1-2a**	**TS 2a-2b**	**TS 2a-3**	**TS 2a-4**	**TS 2a-5a**	**TS 2b-5b**
phenyl	26.6	*a*	46.8	28.6	49.0	*a*
2-furanyl	28.6	*b*	15.8	18.1	*c*	*b*
3-furanyl	28.1	7.4	23.5	25.7	*d*	40.4
2-oxazolyl	23.4	6.7	19.3	22.8	*b*	*c*
4-oxazolyl	36.4	*b*	16.1	18.8	*c*	*b*
5-oxazolyl	34.6	6.8	23.2	25.7	39.9	*b*
1500 K	**TS 1-2a**	**TS 2a-2b**	**TS 2a-3**	**TS 2a-4**	**TS 2a-5a**	**TS 2b-5b**
phenyl	18.7	*a*	44.3	30.1	51.5	*a*
2-furanyl	19.6	*b*	16.0	19.8	*c*	*b*
3-furanyl	19.5	10.3	21.1	27.3	*d*	42.8
2-oxazolyl	13.6	9.8	19.5	24.7	*b*	*c*
4-oxazolyl	26.9	*b*	16.3	20.6	*c*	*b*
5-oxazolyl	24.7	9.7	22.2	27.3	42.0	*b*
2000 K	**TS 1-2a**	**TS 2a-2b**	**TS 2a-3**	**TS 2a-4**	**TS 2a-5a**	**TS 2b-5b**
phenyl	11.0	*a*	42.0	31.8	54.2	*a*
2-furanyl	10.8	*b*	16.5	21.7	*c*	*b*
3-furanyl	11.2	13.5	19.1	29.2	*d*	45.5
2-oxazolyl	4.1	13.2	20.0	26.9	*b*	*c*
4-oxazolyl	17.8	*b*	16.8	22.6	*c*	*b*
5-oxazolyl	15.0	12.9	21.6	29.2	44.4	*b*

[a] Because of symmetry, **2a** = **2b** and **5a** = **5b**. [b] Did not search for this transition state because of irrelevance of the product for energetic reasons or an analogous product is simply not possible. [c] Numerous transition state searches to link the peroxy precursor and each of these dioxetanes resulted in discovery of transition states for the loss of O atom. [d] Despite numerous attempts, this stationary point could not be located at the B3LYP/6-31G* level.

respectively). These values are very similar to the previously reported transition state for O_2 addition to the phenyl radical ($\Delta G^{\ddagger}$(298 K) = 6.1 kcal/mol, $\langle S^2 \rangle$ = 1.76, and 6.2*i* cm^{-1}).[14]

Following the production of the 2- or 3-furanylperoxy radical, cleavage of the O−O bond can occur to yield the aryloxy radical (**3**). There is a significant difference in the energetics of this reaction between the 2- and 3-furanylperoxy radicals. The formation of the 2-furanyloxy radical (**3**) is only slightly endoergic at 298 K (+3.4 kcal/mol), while production of the 3-furanyloxy radical undergoes a free energy penalty of +20.4 kcal/mol at the same temperature. One previously stated explanation for this variance is the enhanced ability for π-delocalization by the 2-furanyloxy radical over the 3-furanyloxy radical (Figure 3).[16]

Multiple transition states have been obtained that link the 2-furanylperoxy radical with several different 2-furanyloxy radicals with O atom complexes. The most stable of these requires a free energy of activation barrier of 16.2 kcal/mol at 298 K (and a 12.8 kcal/mol barrier for the reverse reaction). A 27.3 kcal/mol activation barrier is calculated for the generation of the 3-furanyloxy radical (**3**) via loss of an O atom from the

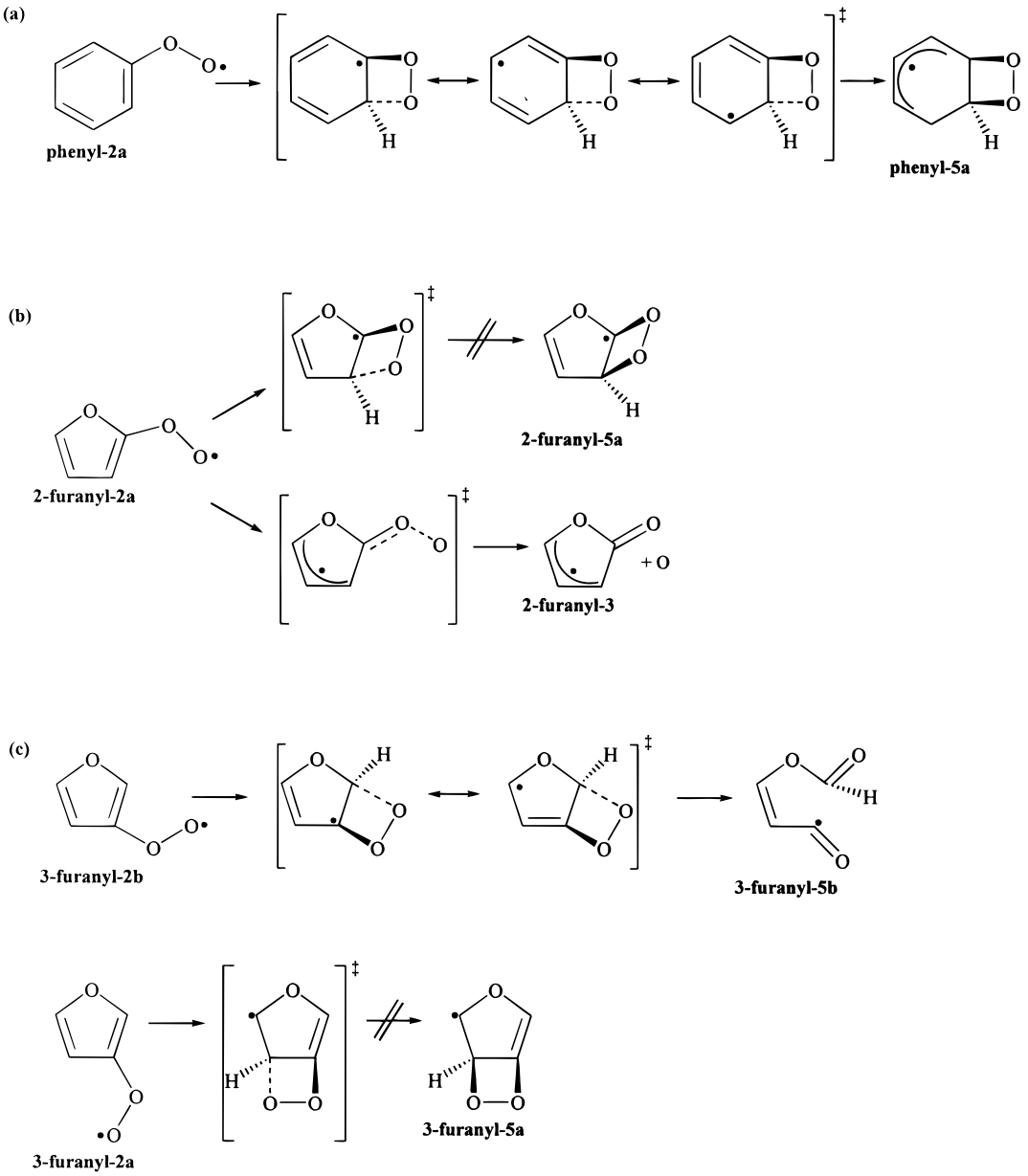

Figure 4. Pictorial representation of the possible unimolecular rearrangements of (a) phenylperoxy, (b) 2-furanylperoxy, and (c) 3-furanylperoxy radicals to yield dioxetanyl intermediates. Transition state geometries with resonance structures are also depicted and marked with ‡.

3-furanylperoxy radical (**2a**). These two transition states differ markedly not only in their energetic values for the forward and reverse reactions but also in the geometry of the respective transition states and the magnitude of their imaginary vibrational frequencies. In the 2-furanyloxy case, the O atom is cleaved perpendicular to the plane of the furan ring and the transition state has an imaginary vibrational frequency of 542*i* cm^{-1}. In the 3-furanyloxy case, the O atom is parallel to the ring with a small imaginary vibrational frequency of only 15*i* cm^{-1}. Both of these transition states suffer from excessive spin contamination with $\langle S^2 \rangle$ values of 1.23 and 1.77 for 2- and 3-furanyloxy radical formation, respectively.

In studying the unimolecular rearrangement of the 2- or 3-furanylperoxy radical, we examined two possible transformations (Figure 3). The bonding of the terminal oxygen to the proximal carbon (1,1-addition) to form the 2- or 3-dioxiranylfuranyl radical (**4**) was examined. The formation of the 2-dioxiranylfuranyl radical possesses a similar free energy of activation barrier at 298 K as cleavage of the O−O bond but is slightly more endoergic for product formation. On the other hand, formation of the 3-dioxiranylfuranyl radical (**2a** → **4**) not only is the more accessible pathway but also is more favorable energetically than O atom loss from the 3-furanylperoxy radical (**2a** → **3**) at 298 K (Tables 1 and 2).

The second rearrangement is the formation of the 2-furanyl-**5a** and 3-furanyl-**5b** dioxetanyl radicals (Figure 3). Although the 2-furanyl-**5a** species was found as a stable minimum using the B3LYP method, all attempts to find a transition state that linked the 2-furanylperoxy radical to the 2-furanyl-**5a** radical failed. Each search resulted in a transition state for the loss of an O atom from the 2-furanylperoxy radical. Two transition states were found that connect to 2-furanyl-**5a** as shown in Figure 3a, but these structures do not link 2-furanyl-**5a** to the 2-furanylperoxy (**2a**) radical.

Two dioxetanyl radicals could result from the unimolecular rearrangement of the 3-furanylperoxy radical (Figure 3b). The 3-furanyl-**5a** radical could not be found using the B3LYP method, and all attempts to maintain the four-membered oxetanyl ring resulted in ring opening and convergence to the 3-furanylperoxy radical. This is not surprising since the 3-fura-

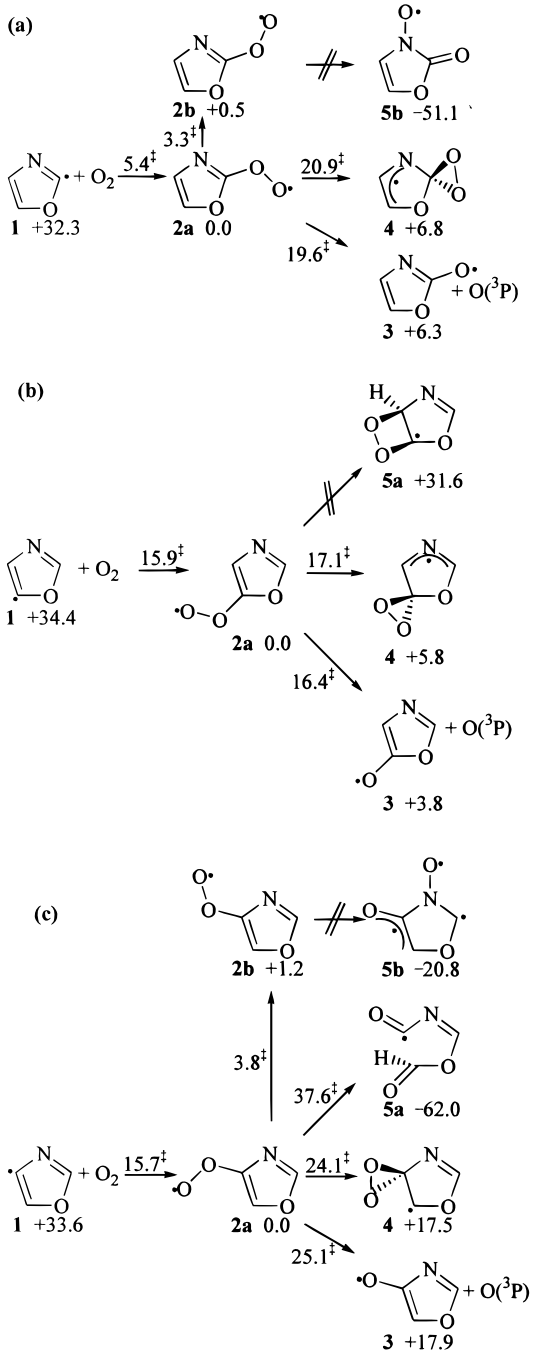

Figure 5. Mechanisms for the (a) 2-oxazolyl + O_2, (b) 4-oxazolyl + O_2, and (c) 5-oxazolyl + O_2 reactions showing Gibbs free energies of activation barriers (relative to the appropriate reactant) and Gibbs free energies of each intermediate at 298 K (relative to the corresponding **2a**) at the B3LYP/6-311+G**//B3LYP/6-31G* level.

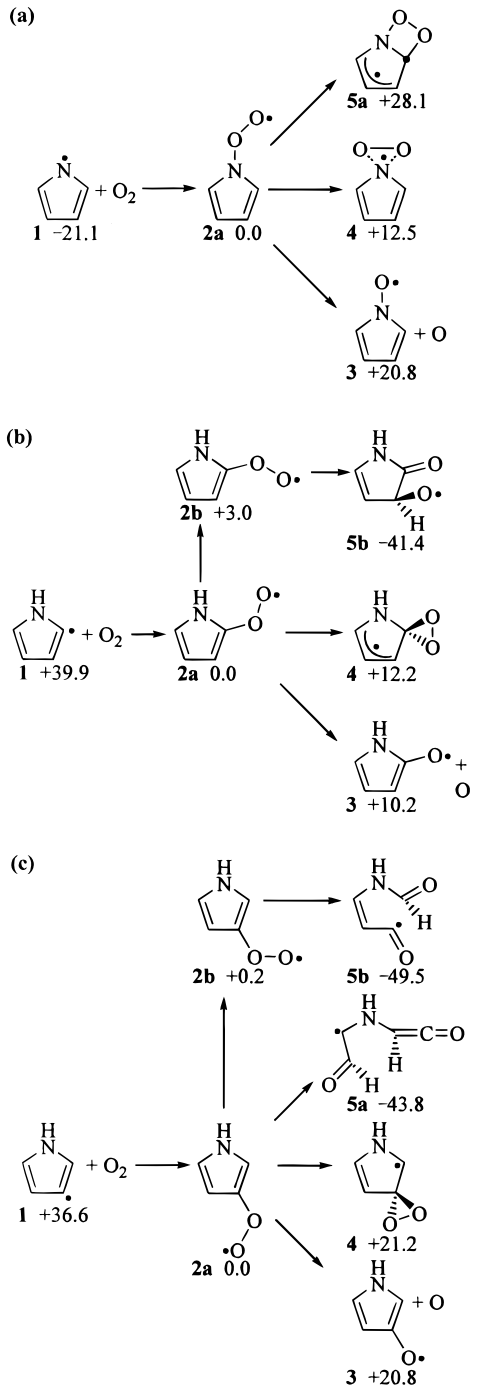

Figure 6. Mechanisms for the (a) pyrrol-1-yl + O_2, (b) pyrrol-2-yl + O_2, and (c) pyrrol-3-yl + O_2 reactions showing Gibbs free energies of each intermediate at 298 K (relative to the corresponding **2a**) at the B3LYP/6-311+G**//B3LYP/6-31G* level.

nyl-**5a** product would be an anti-Bredt[32] bicyclic system, as shown in part c of Figure 4, and would be unable to delocalize effectively the radical's spin density. The only confirmed dioxetanyl transition state for the rearrangement of a furanylperoxy radical results in the production of the 3-furanyl-**5b** radical. The free energy of activation barrier is ∼5−10 kcal/mol lower than that seen in the phenyl[16] or pyridinyl[15] potential energy surfaces for the analogous reactions. The production of the 3-furanyl-**5b** radical is significantly exoergic even though it possesses the highest activation barrier of these considered pathways. This effect is due to the concerted nature of the isomerization where the transfer of an O atom is coupled to the breaking of the C_2-C_3 bond in the 3-furanyl-**5b** radical.

In general, there is a direct correlation between the ability of each system to delocalize the radical center and the discovery of a transition state structure (Figure 4). The phenylperoxy radical readily rearranges to form a dioxetanyl intermediate, yet no transition state has been discovered that links the 2-furanylperoxy radical (**2a**) with 2-furanyl-**5a**. However, the connection of the 3-furanylperoxy radical to 3-furanyl-**5b** has been established (Figure 4c). This transition state and the one for phenylperoxy radical rearrangement can effectively delocalize the radical around the ring, while the 2-furanylperoxy radical is not afforded this ability. In what has been seen in the furanyl and will be shown in the oxazolyl system, dioxetane formation

TABLE 3: Relative Energies (kcal/mol) at Different Theoretical Levels for a Few Important Intermediates and Transition States on the Potential Energy Surface of 3-furanylperoxy and 5-oxazolylperoxy Radicals[a]

3-furanylperoxy radical	**2a**	**TS 1-2a**	**TS 2a-2b**	**TS 2a-3**	**TS 2a-4**	**TS 2b-5b**
UMP2/6-31G**	0.0	44.9	−5.0	54.8	26.0	56.4
UMP3/6-31G**	0.0	46.2	−3.6	43.7	26.7	51.6
UMP4(SDQ)/6-31G**	0.0	44.8	−1.6	44.0	26.3	48.1
UCCSD/6-31G**	0.0	44.1	2.0	35.3[b]	25.5	38.6
UCCSD(T)/6-31G**	0.0	45.6	2.4	*b*	24.0	35.8
UB3LYP/6-311+G**	0.0	47.9	4.1	31.1	25.5	38.5
UB3LYP/6-31G*	0.0	50.2	4.5	35.3	25.5	38.2
UB3LYP/6-311+G** $\langle S^2\rangle$	0.76	1.77	0.75	1.77	0.77	0.78
UCCSD(T)/6-31G** $\langle S^2\rangle$	0.95	2.16	0.77	2.02	1.09	1.41
5-oxazolylperoxy radical	**2a**	**TS 1-2a**	**TS 2a-2b**	**TS 2a-3**	**TS 2a-4**	**TS 2a-5a**
UMP2/6-31G**	0.0	48.0	2.5	39.0	29.3	64.4
UMP3/6-31G**	0.0	49.0	1.8	28.2	29.2	57.5
UMP4(SDQ)/6-31G**	0.0	47.1	2.4	28.4	28.5	53.2
UCCSD/6-31G**	0.0	45.1	2.6	25.7[b]	26.8	40.3
UCCSD(T)/6-31G**	0.0	46.3	2.8	*b*	25.0	37.0
UB3LYP/6-311+G**	0.0	57.2	3.5	28.0	25.3	38.7
UB3LYP/6-31G*	0.0	60.0	4.1	32.2	25.4	38.3
UB3LYP/6-311+G** $\langle S^2\rangle$	0.76	1.76	0.75	1.49	0.77	0.78
UCCSD(T)/6-31G** $\langle S^2\rangle$	0.87	2.11	0.86	1.93	1.04	1.44

[a] The B3LYP/6-31G* geometry was used in each case. The relative energies are at the bottom-of-the-well. [b] The CCSD equations could not be converged to the necessary accuracy ($<10^{-7}$ au) by Gaussian 98 in order to complete the UCCSD(T) calculation. The corresponding CCSD energy for **TS 2a-3** reflects a 10^{-5} au convergence.

appears to be significantly dependent on delocalization of the radical in the intermediate and also in the transition state.

C. Comparison to the Oxazolyl Radical + O_2 Reaction Mechanism. The oxidation of 2-, 4-, and 5-oxazolyl radicals and further rearrangement was studied to determine the effect of a second heteroatom within a five-membered ring (Figure 2). In particular, oxazole allows for an examination of the effect of N, O, or both heteroatoms on the relative rearrangement pathways. For instance, the 5-position of oxazole is ortho only to N, while the 4-position is ortho only to O. The 2-position is ortho to both N and O, and a mechanistic analysis allows for an examination of any synergistic effects. However, in general, the energetics of the intermediates and transition states of the oxazolylperoxy radical (**2**) are very well correlated with those for the furanylperoxy radicals (Tables 1 and 2).

The rearrangement of the 2- and 4-oxazolylperoxy radicals closely follow all of the major trends seen in the 2-furanylperoxy radical's rearrangements (Figure 5). For both 2- and 4-oxazolylperoxy radicals, the least endoergic reaction at 298 K is the loss of an O atom to yield the 2- and 4-oxazolyloxy (**3**) radicals. The cleavage of the O−O bond also has the lowest calculated free energy of activation barrier ($\Delta G^{\ddagger}$, 298 K), but these calculations are suspect due to the excessive spin contamination. The presence of the N atom in the ring raises slightly the calculated energies at the 2-position compared to the 4-position or even those of the 2-furanyl system. Another similarity is seen in the search for transition states that lead to formation of the possible dioxetanyl radicals, 2-oxazolyl-**5b** and 4-oxazolyl-**5a**. In both cases, all attempts failed; transition states found during these searches linked the 2- and 4-oxazolylperoxy radicals to 2- and 4-oxazolyloxy (**3**) radicals.

The 5-oxazolylperoxy radical pathways mirror that of the 3-furanylperoxy radical (Figure 5c). The activation barriers and endoergicities are slightly lowered for the reactions that form the 5-oxazolyloxy radical (**3**) and the 5-dioxiranyloxazolyl radical (**4**) as compared to the 3-furanylperoxy potential energy surface. In general, the 5-oxazolylperoxy radical has higher barriers for rearrangement as compared to the 2- and 4-oxazolylperoxy radicals. However, for both 3-furanylperoxy and 5-oxazolylperoxy radicals, the dioxiranyl pathways are favored at 298 K over all of the other rearrangements examined.

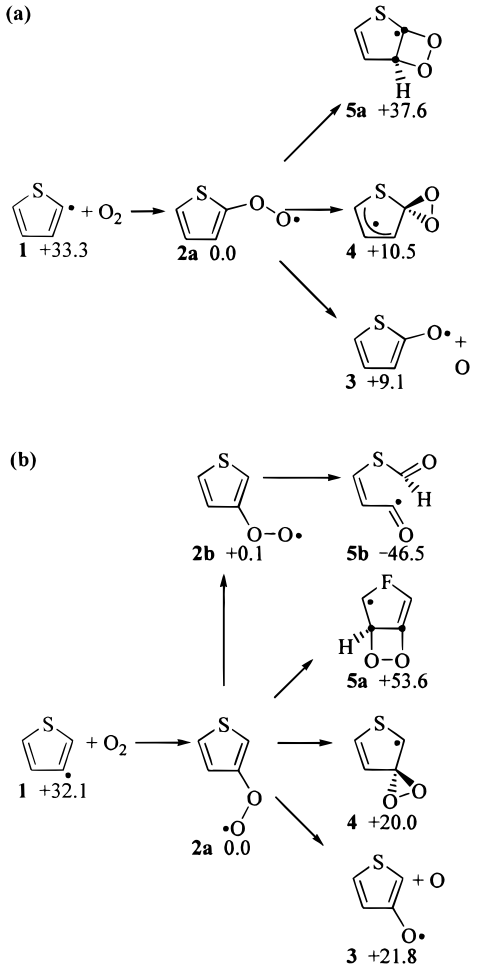

Figure 7. Mechanisms for the (a) thiophen-2-yl + O_2 and (b) thiophen-3-yl + O_2 reactions showing Gibbs free energies of each intermediate at 298 K (relative to the corresponding **2a**) at the B3LYP/6-311+G**// B3LYP/6-31G* level.

D. Comparison of Theoretical Levels. We also calculated single point energies at the UCCSD(T)/6-31G** level for the 3-furanylperoxy radical, 5-oxazolylperoxy radical, and their

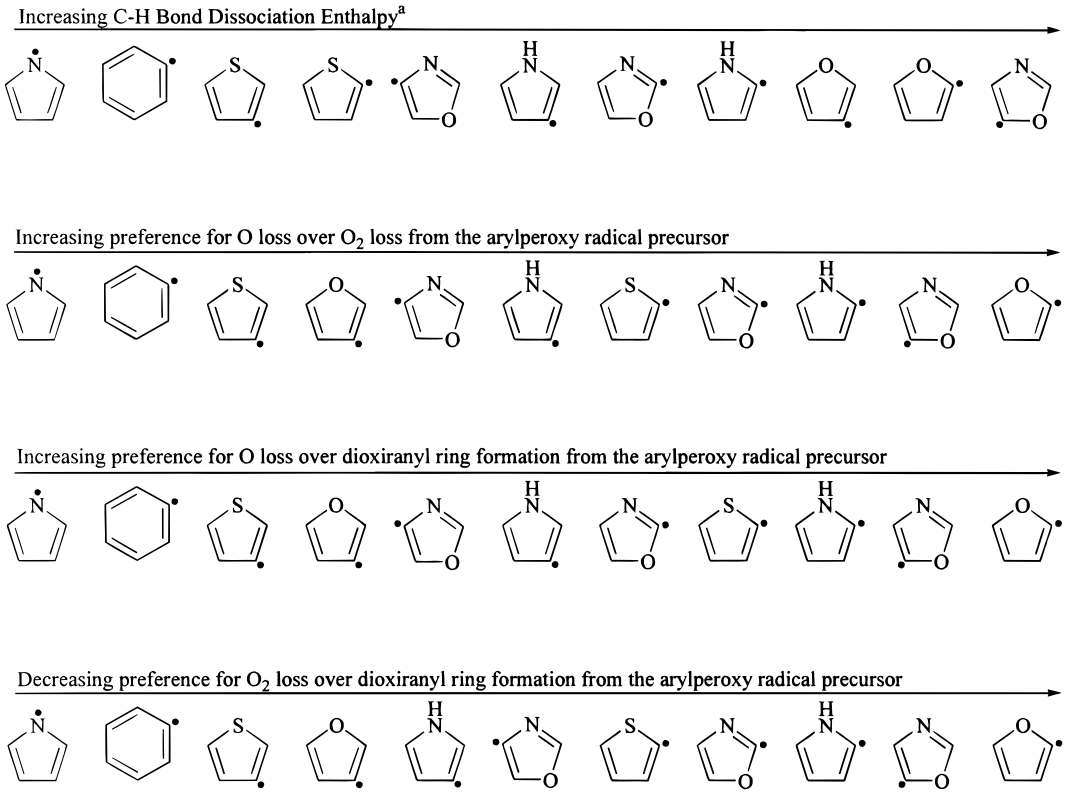

Figure 8. Observed trends of five-membered heterocyclic radical oxidation and further rearrangements as compared to the related C−H BDE in the parent aromatic ring. [a]See ref 24.

transition states for rearrangement in order to evaluate the quantitative accuracy of the B3LYP energies. These relative energies (at the bottom of the well) are provided in Table 3. The UCCSD(T) energies are in good qualitative and quantitative agreement with the B3LYP results (within ~3 kcal/mol). Because of the high level of spin contamination for the UHF reference wave function, the 3-furanyl-**TS 2a-3** and the 5-oxazolyl-**TS 2a-3** calculations at the UCCSD(T) level failed to converge the coupled-cluster equations. However, overall there is general consensus between the B3LYP and UCCSD(T) energies.

E. Comparison of Reaction Pathways as a Function of Temperature. Upon observing the changes in relative Gibbs free energy as the temperature increases from 298 to 2000 K, several trends become evident (Tables 1 and 2). At temperatures <1500 K, the addition of O_2 to the furanyl or oxazolyl radicals is exoergic, which demonstrates that the formation of the arylperoxy intermediate is thermodynamically favorable across a wide range of temperatures. At temperatures >1500 K, if the arylperoxy radical intermediate is formed, then the simple decomposition of arylperoxy to aryl radical and O_2 has the lowest activation barrier, except for the 4-oxazolylperoxy radical.

Another important trend is the proclivity of the arylperoxy radicals derived from the five-membered rings to lose an O atom at temperatures ≥500 K. In general, the furanyloxy and oxazolyloxy radicals (**3**) are the most stable intermediates from 500 to 2000 K, except for a few dioxetanyl radical species. These dioxetanyl radicals include 3-furanyl-**5b**, 2-oxazolyl-**5b,** 5-oxazolyl-**5a**, and 5-oxazolyl-**5b** (Figures 3−5); however, in these peculiar cases, either the activation barriers for formation of the oxetanyl radicals are at least 10 kcal/mol higher than the loss of O atom or transition states were not found for the direct conversion of the peroxy radical precursor to yield the dioxetanyl radical intermediate. The production of the dioxiranyl radical intermediates is only favored kinetically or thermodynamically at low temperatures (≤500 K) for the 3-furanyl and 5-oxazolyl potential energy surfaces.

F. Other Five-Membered Rings: Pyrrole and Thiophene. We also calculated the analogous intermediates (but not their respective transition states) for the pyrrolyl and thiophenyl radicals (Table 1 and Figures 6 and 7). When the energetics for these systems are compared with those of the phenyl, furanyl, and oxazolyl radicals, several trends become evident. These trends are shown schematically in Figure 8. The trends are consistently related to the position of the radical center relative to the heteroatom (2- vs 3-position) as well as the magnitude of the C−H bond dissociation enthalpy (BDE) for generating the carbon-centered radical.[24]

In general, the preference for the loss of O atom over the loss of O_2 from the five-membered arylperoxy radical precursor increases for arylperoxy radicals derived from the 2-position over the 3-position, and within these subsets, the preference increases with respect to increasing C−H BDE. The only five-membered arylperoxy radical in this study that prefers O_2 loss over O loss at all temperatures is the pyrrol-1-ylperoxy radical (**2a**) (derived from the N-centered radical). This is due to the unique stability of the pyrrol-1-yl radical (Figure 6), as this radical, like the cyclopentadienyl radical, has the unpaired electron in the π-system—for a total of 5 electrons in the π-system.[24,33,34] Most carbon-centered aryl radicals have the unpaired electron in the σ-system.[24]

The same trend is seen for the relative stability of dioxiranylaryl radicals (**4**) as compared to aryloxy radicals (**3**). At 298 K, all peroxy radicals derived from the 2-position favor O atom loss over isomerization to the dioxiranyl product, except for the 5-oxazolylperoxy radical. By 500 K, the aryloxy radical intermediate is more stable than every corresponding dioxiranyl radical intermediate except in the case of the pyrrol-1-ylperoxy radical.

Finally, dioxetanyl radical products resulting from the rearrangement of pyrrolylperoxy and thiophenylperoxy radicals have been explored (Figures 6 and 7). Only three bicyclic structures were converged to be stable minima using the B3LYP method: pyrrol-1-yl-**5a**, thiophen-2-yl-**5a**, and thiophen-3-yl-**5a**. All of the other structures exhibited O−O bond scission, a C−C bond cleavage, or a combination of both. It is doubtful that transition state structures can be found that directly link the parent peroxy intermediate to either pyrrol-2-yl-**5b** or pyrrol-3-yl-**5a** dioxetanyl radicals based on our previously noted observations in the furanyl and oxazolyl potential energy surfaces. With regard to the dioxetanyl radicals derived from the thiophenyl system, it is highly likely that direct linkage between the thiophenylperoxy radical and each dioxetanyl radical may exist due to the increased polarizability of sulfur as compared to oxygen.

IV. Conclusions

We have explored the potential energy surfaces, including transition states, for the reaction and subsequent rearrangement of O_2 addition to furanyl and oxazolyl radicals. Thermodynamic comparisons have been presented for these systems with the thiophenyl and pyrrolyl radical systems. A range of temperatures relevant to both atmospheric and combustion processes have been explored for all of these reaction mechanisms.

Throughout the five-membered ring heterocycles, the formation of the aryloxy intermediate is generally the most favored intermediate evolving from the arylperoxy radical. This preference is greater than that observed in the phenylperoxy radical[14,16] or other six-membered ring heterocycles.[15] The thermodynamic stability and activation barriers for formation of the dioxiranyl intermediates are comparable to the aryloxy intermediates at low temperatures. However, the dioxetanyl radical intermediates are much less favored. If the dioxetanyl radicals demonstrate more stability than their aryloxy counterparts, they suffer kinetically with higher activation barriers or the lack of a direct pathway (i.e., no transition state) for formation from the initial arylperoxy radical intermediate.

Acknowledgment. We gratefully acknowledge the U.S. Department of Energy (Grant DE-FG22-96PC96249), the Ohio Supercomputer Center, and the U.S. Army for support of this research. We also thank Paul R. Rablen (Swarthmore College) for providing his Thermo94 program.

Supporting Information Available: Energies, enthalpies, free energies as a function of temperature, and moments of inertia for all intermediates and transition states for the reaction of each aryl radical with O_2. Cartesian coordinates and harmonic frequencies for all intermediates and transition states for each aryl radical with O_2. This material is available free of charge via the Internet at http://pubs.acs.org.

References and Notes

(1) (a) Smith, K. L.; Smoot, L. D.; Fletcher, T. H.; Pugmire, R. J. *The Structure and Reaction Processes of Coal*; Plenum Press: New York, 1994. (b) Meyers, R. A. *Coal Structure*; Academic Press: New York, 1982.

(2) Brezinsky, K. *Prog. Energy Combust. Sci.* **1986**, *12*, 1−24.

(3) Bittker, D. A. *Combust. Sci. Technol*. **1991**, *79*, 49−72.

(4) Colussi, A. J.; Zabel, F.; Benson, S. W. *Int. J. Chem. Kinet*. **1977**, *9*, 161−178.

(5) Zhang, H.-Y.; McKinnon, J. T. *Combust. Sci. Technol*. **1995**, *107*, 261−300.

(6) Chai, Y.; Pfefferle, L. D. *Fuel* **1998**, *77*, 313−320.

(7) Morris, V. R.; Bhatia, S. C.; Stelson, A. W.; Hall, J. H. *Energy Fuels* **1991**, *5*, 126−133.

(8) Fulle, D.; Dib, A.; Kiefer, J. H.; Zhang, Q.; Yao, J.; Kern, R. D. *J. Phys. Chem. A* **1998**, *102*, 7480−7486.

(9) Organ, P. P.; Mackie, J. C. *J. Chem. Soc., Faraday Trans.* **1991**, *87*, 815−23.

(10) Lifshitz, A.; Bidani, M.; Bidani, S. *J. Phys. Chem.* **1986**, *90*, 5373−5377.

(11) Grela, M. A.; Amorebieta, V. T.; Colussi, A. J. *J. Phys. Chem.* **1985**, *89*, 38−41.

(12) Lifshitz, A.; Tamburu, C.; Suslensky, A. *J. Phys. Chem.* **1989**, *93*, 5802−5808.

(13) Sendt, K.; Bacskay, G. B.; Mackie, J. C. *J. Phys. Chem. A* **2000**, *104*, 1861−1875.

(14) Fadden, M. J.; Barckholtz, C.; Hadad, C. M. *J. Phys. Chem. A* **2000**, *104*, 3004−3011.

(15) Fadden, M. J.; Hadad, C. M. *J. Phys. Chem. A* **2000**, *104*, 6088.

(16) Barckholtz, C.; Fadden, M. J.; Hadad, C. M. *J. Phys. Chem. A* **1999**, *103*, 8108−8117.

(17) Frisch, M. J.; Trucks, G. W.; Schlegel, H. B.; Gill, P. M. W.; Johnson, B. G.; Robb, M. A.; Cheeseman, J. R.; Keith, T.; Petersson, G. A.; Montgomery, J. A.; Raghavachari, K.; Al-Laham, M. A.; Zakrzewski, V. G.; Ortiz, J. V.; Foresman, J. B.; Peng, C. Y.; Ayala, P. Y.; Chen, W.; Wong, M. W.; Andres, J. L.; Replogle, E. S.; Gomperts, R.; Martin, R. L.; Fox, D. J.; Binkley, J. S.; Defrees, D. J.; Baker, J.; Stewart, J. J. P.; Head-Gordon, M.; Gonzalez, C.; Pople, J. A. *Gaussian 94*, Revision D.3; Gaussian, Inc.: Pittsburgh, PA, 1995.

(18) Frisch, M. J.; Trucks, G. W.; Schlegel, H. B.; Scuseria, G. E.; Robb, M. A.; Cheeseman, J. R.; Zakrzewski, V. G.; Montgomery, J. A. Jr.; Stratmann, R. E.; Burant, J. C.; Dapprich, S.; Millam, J. M.; Daniels, A. D.; Kudin, K. N.; Strain, M. C.; Farkas, O.; Tomasi, J.; Barone, V.; Cossi, M.; Cammi, R.; Mennucci, B.; Pomelli, C.; Adamo, C.; Clifford, S.; Ochterski, J.; Petersson, G. A.; Ayala, P. Y.; Cui, Q.; Morokuma, K.; Malick, D. K.; Rabuck, A. D.; Raghavachari, K.; Foresman, J. B.; Cioslowski, J.; Ortiz, J. V.; Stefanov, B. B.; Liu, G.; Liashenko, A.; Piskorz, P.; Komaromi, I.; Gomperts, R.; Martin, R. L.; Fox, D. J.; Keith, T.; Al-Laham, M. A.; Peng, C. Y.; Nanayakkara, A.; Gonzalez, C.; Challacombe, M.; Gill, P. M. W.; Johnson, B.; Chen, W.; Wong, M. W.; Andres, J. L.; Gonzalez, C.; Head-Gordon, M.; Replogle, E. S.; Pople, J. A. *Gaussian 98*, Revision A.7; Gaussian, Inc.: Pittsburgh, PA, 1998.

(19) (a) Labanowski, J. W.; Andzelm, J. *Density Functional Methods in Chemistry*; Springer: New York, 1991. (b) Parr, R. G.; Yang, W. *Density Functional Theory in Atoms and Molecules*; Oxford University Press: New York, 1989.

(20) Becke, A. D. *Phys. Rev. A* **1988**, *38*, 3098−3100.

(21) Lee, C.; Yang, W.; Parr, R. G. *Phys. Rev. B.* **1988**, *37*, 785−789.

(22) Becke, A. D. *J. Chem. Phys.* **1993**, *98*, 1372.

(23) Hehre, W. J.; Radom, L.; Schleyer, P. v. R.; Pople, J. A. *Ab Initio Molecular Orbital Theory*; John Wiley & Sons: New York, 1986.

(24) Barckholtz, C.; Barckholtz, T. A.; Hadad, C. M. *J. Am. Chem. Soc.* **1999**, *121*, 491−500.

(25) (a) Cioslowski, J.; Liu, G.; Martinov, M.; Piskorz, P.; Moncrieff, D. *J. Am. Chem. Soc.* **1996**, *118*, 5261−5264. (b) Cioslowski, J.; Liu, G.; Moncrieff, D. *J. Org. Chem.* **1996**, *61*, 4111−4114.

(26) Bauschlicher, C. W., Jr.; Langhoff, S. R. *Mol. Phys.* **1999**, *96*, 471.

(27) Stanton, J. F.; Gauss, J.; Watts, J. D.; Lauderdale, W. J.; Bartlett, R. J. *Int. J. Quantum Chem.* **1992**, *S26*, 879.

(28) Scott, A. P.; Radom, L. *J. Phys. Chem.* **1996**, *100*, 16502−16513.

(29) (a) Gonzalez, C.; Schlegel, H. B. *J. Chem. Phys.* **1989**, *90*, 2154. (b) Gonzalez, C.; Schlegel, H. B. *J. Phys. Chem.* **1990**, *94*, 5523.

(30) Rablen, P. R. *Thermo94*, Yale University, 1994.

(31) Chase, M. W., Jr. *NIST-JANAF Thermochemical Tables*; American Institute of Physics for the National Institute of Standards and Technology: New York, 1998.

(32) Bredt, J.; Thouet, H.; Schmitz, J. *Liebigs Ann. Chem.* **1924**, *437*, 1.

(33) Blank, D. A.; North, S. W.; Lee, Y. T. *Chem. Phys.* **1994**, *187*, 35−47.

(34) Backsay, G. B.; Martoprawiro, M.; Mackie, J. C. *Chem. Phys. Lett.* **1998**, *290*, 391−398.